
A BAYESIAN HIERARCHICAL GENERALIZATION OF EMPIRICAL BAYES FOR CRASH RATE ESTIMATION WITH MISSING TRAFFIC VOLUME

A PREPRINT

✉ **Lars Skaug**
larsiskaug@gmail.com

May 2026

ABSTRACT

The Empirical Bayes (EB) procedure of Hauer et al. (2002) is the workhorse of highway safety analysis: it combines a Safety Performance Function with observed crash counts to produce shrinkage estimates of segment-level crash rates. EB delivers practicality by holding several quantities fixed at calibration: SPF coefficients, per-type overdispersion, observed ADT, and a fixed exposure exponent. These assumptions strain when ADT is missing on a majority of segments. We present a fully Bayesian hierarchical model that generalizes EB by relaxing each of these assumptions in a single joint inference. Fit on Ohio’s road inventory (408,304 segments, 2.9 million crashes, 2013–2025), the model jointly imputes missing ADT and estimates per-segment crash rates with uncertainty. Posterior predictive checks of an initial fixed-exposure model expose a tail misfit; relaxing the exposure structure to a per-functional-class exposure exponent and an estimated length exponent, in place of a single scalar and a fixed offset, resolves it and improves out-of-sample predictive accuracy (PSIS-LOO $\Delta\text{elpd} = 9,394$, SE 238). Crash count is sublinear in traffic in every class (exposure exponents 0.49–0.70, all < 1 , the safety-in-numbers effect) and sublinear in segment length ($\beta_{\text{len}} = 0.69$). Partial pooling substantially improves out-of-sample predictive accuracy over complete pooling (PSIS-LOO $\Delta\text{elpd} = 4,780$, SE 225). On equal features, the Bayesian ADT submodel attains $R_{\log}^2 = 0.756$ versus 0.653 for LightGBM. The output is a posterior crash rate distribution per segment, replacing the median-by-type point estimates used in our prior risk-aware routing framework.

Keywords Empirical Bayes · Bayesian hierarchical model · crash rate estimation · AADT imputation · partial pooling · road safety

1 Introduction

Empirical Bayes (EB), as introduced for highway safety by Hauer et al. (2002), combines a Safety Performance Function (SPF) with observed crash counts to produce shrinkage estimates of segment-level crash rates. Of the many methods, data sources, and emerging techniques available for crash analysis (Skaug et al., 2025), EB is the one codified in the AASHTO Highway Safety Manual and routinely used by state DOTs to identify high-risk segments, prioritize improvements, and evaluate safety treatments.

EB delivers practicality by holding several quantities fixed at calibration. The SPF coefficients are point estimates; overdispersion is one parameter per road type; ADT enters as a known covariate; and the exposure exponent is fixed during SPF fitting. These choices are deliberate and appropriate when the assumptions hold. They strain when ADT is missing on most segments, when road types are heterogeneous within a class, and when downstream applications such as risk-aware routing require uncertainty quantification.

This paper presents a fully Bayesian hierarchical model that generalizes EB by relaxing those fixed-parameter assumptions in a single joint inference, enabled by modern MCMC. We fit it on Ohio’s road inventory: 408,304 segments

across 7 functional classes, joined to 2,937,455 geocoded crashes from 2013–2025. ADT is observed on 128,021 segments (31%) and latent on the remaining 280,283.

The paper builds on Skaug and Nojoumian (2026), which introduced a risk-aware routing framework using a frequentist LightGBM ADT model and median-by-type crash rates. Three limitations identified in that paper motivate the present work: ADT is imputed without uncertainty propagation; crash rates assume linear exposure; and rates are computed by simple medians with no borrowing of strength across similar segments. We address each directly. The present paper is self-contained: Section 2 gives the EB background needed to read it without the prior paper, and the routing application is summarized rather than reproduced.

The contributions are:

1. A joint Bayesian hierarchical model for crash counts that treats missing ADT as a latent variable, propagates exposure uncertainty into rate estimates end-to-end, and estimates the exposure exponent from data rather than fixing it at calibration.
2. An ADT submodel that, on equal features, outperforms a LightGBM baseline ($R_{\log}^2 = 0.756$ vs. 0.653).
3. A generative-simulation comparison showing that the standard two-stage Bayesian multiple-imputation alternative (Rubin, 1987) introduces material bias in the exposure exponent (-0.311) by severing the crash-to-ADT likelihood feedback.
4. Segment-level posterior crash rates with 94% credible intervals for all 408,304 inventory segments, suitable as drop-in replacements for the categorical median rates used in the prior routing framework.

2 Background: Empirical Bayes and Its Fixed Assumptions

EB combines two pieces of information about a road segment i : a Safety Performance Function estimate μ_i for “similar” entities (typically $\mu_i = \alpha \cdot \text{ADT}_i^\beta$ for a given road class), and the observed crash count y_i on that segment. The EB estimate of the expected crash count is the weighted average

$$\hat{\lambda}_i^{\text{EB}} = w_i \mu_i + (1 - w_i) y_i, \quad w_i = \frac{1}{1 + \mu_i / \phi}, \quad (1)$$

where ϕ is the negative-binomial overdispersion parameter (Hauer et al., 2002). Concretely, a one-mile rural arterial with predicted $\mu = 4$ crashes/year, observed $y = 12$, and $\phi = 5$ yields $w = 5/9 \approx 0.56$ and $\hat{\lambda}^{\text{EB}} \approx 0.56 \cdot 4 + 0.44 \cdot 12 = 7.5$ crashes/year. The shrinkage pulls rare-event segments toward their group mean and leaves crash-rich segments closer to their observed counts.

Equation (1) has a Bayesian reading. Under a Gamma($\mu_i/\phi, 1/\phi$) prior on the segment’s latent rate and a Poisson likelihood for the count, the posterior mean is exactly $\hat{\lambda}_i^{\text{EB}}$ and w_i is the posterior weight on the prior. EB and full Bayes share this foundation. Where they differ is in what is held fixed. EB delivers practicality by making five such fixed-parameter assumptions:

1. The SPF coefficients (α, β) are point estimates, fit by maximum likelihood at calibration.
2. The overdispersion parameter ϕ is a single number per road type.
3. ADT enters as a known covariate.
4. The exposure exponent β is fixed during SPF calibration, often near 0.5–0.7 for rural roads and at 1 for the simpler proportional form.
5. The output is the point estimate $\hat{\lambda}_i^{\text{EB}}$, not a distribution.

Each assumption is appropriate when it holds. Closed-form weights and type-level SPFs are precisely what makes EB usable in a spreadsheet, and that accessibility is a feature, not a bug.

The present paper relaxes the five assumptions in a single joint posterior. The intent is computational evolution rather than correction: EB remains the right tool where its assumptions hold (we return to this in Section 6.2). As a preview, the data-estimated exposure exponents are sublinear in every functional class (0.49–0.70), consistent with Hauer’s safety-in-numbers regime, but pinned to posterior intervals rather than a single chosen value, and free to differ by class.

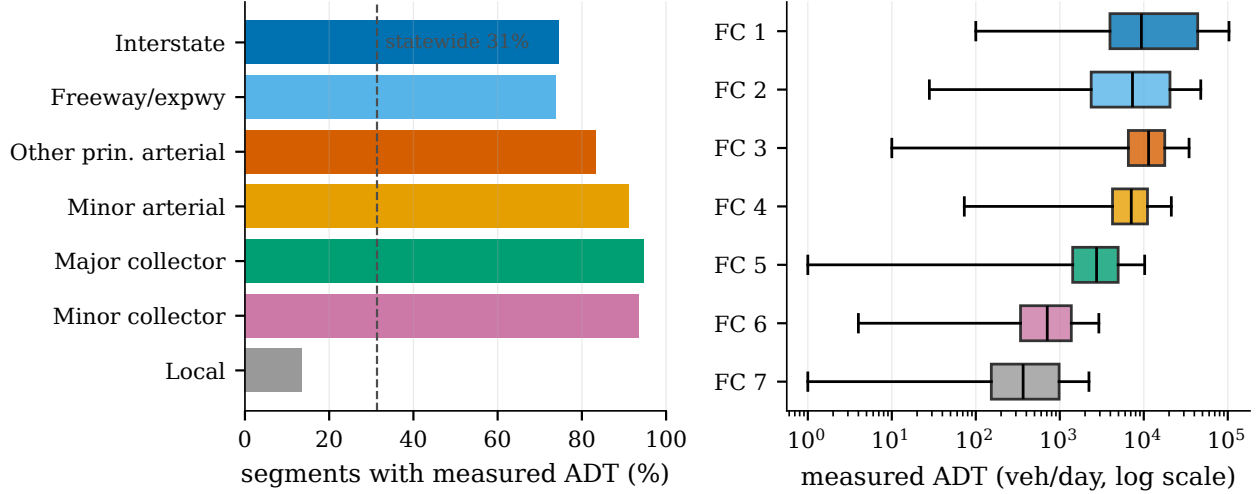


Figure 1: ADT measurement coverage is far from uniform across functional class. Left: share of segments with measured ADT by class, against the statewide 31% rate; higher-class roads are nearly fully measured while local roads (the bulk of the inventory) are largely not, which is what drives the low overall rate. Right: distribution of measured ADT by class (log scale), showing the classes separate in level as well as in coverage.

3 Data

We use three Ohio DOT datasets: the road inventory (408,304 segments with attributes including functional class, lane count, roadway and surface widths, posted speed limit, and county); the traffic count segments (ADT measured on 128,021 segments, 31%, with coverage highly non-uniform across functional class, Figure 1); and 2,937,455 geocoded crash records from 2013–2025 obtained from ODOT’s GCAT export. Crashes are joined to inventory segments via the linear reference system (NLF_ID plus control section), so the geometry and the crash records share a single coordinate space.

This linear-reference join is the one substantive change from the data pipeline of Skaug and Nojournian (2026), which matched crash points to OSM ways through a buffer-and-overlap procedure that introduced cross-dataset alignment errors. Working directly in the inventory’s coordinate space removes that buffer-radius dependence. The broader problem of validating and correcting such geospatial inventory data is treated in Skaug and Nojournian (2025).

The feature set comprises three categorical attributes (functional class, county, and an urban/rural area code) and four standardized continuous predictors (number of through lanes, posted speed limit, total roadway width, and surface width on the left of the centerline). Functional class has 7 levels; county has 88. The continuous features are drawn from the inventory’s design-attribute fields and are present on every segment. Functional class anchors both submodels: it groups the SPF and indexes hierarchical intercepts and slopes. Urban/rural enters the crash submodel only, to close the lane-count backdoor (urban areas have both more lanes and higher crash density). Two attributes flagged as predictive in the prior paper’s tree-based EDA are deliberately omitted: route type, which is collinear with functional class (interstates are FC 1, US highways FC 2–3, county roads FC 6–7); and route number, whose hundreds of unique values make it impractical for a Bayesian regression but which is partly absorbed by the county random effect.

4 Model

4.1 ADT Submodel

The ADT submodel is a hierarchical log-linear regression. For segment i with measured ADT,

$$\log(\text{ADT}_i) \sim \mathcal{N}(\eta_i^{\text{adt}}, \sigma_{\text{adt}}), \tag{2}$$

$$\eta_i^{\text{adt}} = \mathbf{z}_i^\top \boldsymbol{\beta}_{\text{adt}} + \mathbf{z}_i^\top \boldsymbol{\beta}_{\text{adt}, \text{fc}[i]}^{\text{dev}} + \mathbf{z}_i^{(2)\top} \boldsymbol{\gamma}_{\text{adt}} + \delta_{\text{county}[i]} + \delta_{\text{fc}[i]}, \tag{3}$$

where \mathbf{z}_i is the vector of standardized continuous predictors (lanes, speed limit, roadway width, surface width left), $\boldsymbol{\beta}_{\text{adt}}$ are global slopes, $\boldsymbol{\beta}_{\text{adt}, \text{fc}}^{\text{dev}}$ are FC-level slope deviations under a non-centered parameterization, $\mathbf{z}_i^{(2)}$ holds the squared standardized predictors for quadratic curvature, and $\delta_{\text{county}}, \delta_{\text{fc}}$ are random intercepts. Priors are weakly informative:

$\beta_{\text{adt}} \sim \mathcal{N}(0, 5)$, $\sigma_{\text{adt}} \sim \text{HalfNormal}(2)$, $\sigma_{\text{county}} \sim \text{HalfNormal}(2)$, $\sigma_{\text{fc}} \sim \text{HalfNormal}(5)$. The wider hyperprior on σ_{fc} was chosen after an initial run with $\text{HalfNormal}(1)$ produced a posterior concentrating at ~ 4.4 and severe convergence failure; this is recorded honestly because the correction is itself a useful artefact for replicators.

We compare this submodel to a LightGBM regressor on the same four continuous features using identical 5-fold out-of-fold splits. The Bayesian model attains $R_{\text{log}}^2 = 0.756$ with residual standard deviation 0.850 on the log scale; LightGBM attains $R_{\text{log}}^2 = 0.653$ with residual standard deviation 1.014. The prior paper reported a higher LightGBM R^2 (0.877), but that result used 8 features including the high-cardinality categorical (county, route type) that here are absorbed by the hierarchical intercepts. On equal features, the partial-pooling structure beats the boosted-tree baseline; the hierarchical intercepts are doing the work that a tree model would otherwise have to learn through deep splits.

4.2 Joint Crash + ADT Model

The crash submodel is a negative binomial regression for the count y_i :

$$y_i \sim \text{NegBinom}(\mu_i, \alpha_{\text{fc}[i]}), \quad (4)$$

$$\begin{aligned} \log \mu_i = & \beta_{0, \text{fc}[i]} + \beta_{1, \text{fc}[i]} \cdot \text{lanes}_i^z + \beta_2 \cdot \text{urban}_i + \beta_3 \cdot \text{speed}_i^z + \beta_4 \cdot \text{rdwy}_i^z + \beta_5 \cdot \text{surf}_i^z \\ & + \log(365 \cdot T) + \beta_{\text{len}} \cdot \log(L_i) + \beta_{\text{exp}, \text{fc}[i]} \cdot \log(\text{ADT}_i), \end{aligned} \quad (5)$$

where L_i is segment length in miles, $T = 13$ years, and z superscripts denote standardization. Group intercepts and lane slopes are partially pooled: $\beta_{0, \text{fc}} \sim \mathcal{N}(\mu_{\beta_0}, \sigma_{\beta_0})$ and $\beta_{1, \text{fc}} \sim \mathcal{N}(\mu_{\beta_1}, \sigma_{\beta_1})$, with the centered parameterization (appropriate for 7 well-populated FC groups). The exposure exponent is likewise partially pooled across functional class, $\beta_{\text{exp}, \text{fc}} \sim \mathcal{N}(\mu_{\beta_{\text{exp}}}, \sigma_{\beta_{\text{exp}}})$ with $\mu_{\beta_{\text{exp}}} \sim \mathcal{N}(1, 0.3)$, centered at proportionality but admitting a sublinear posterior, and free to differ by class. Per-FC overdispersion $\alpha_{\text{fc}} \sim \text{HalfNormal}(2)$. Fixed-effect slopes have priors $\beta_{2..5} \sim \mathcal{N}(0, 0.5)$ and the length exponent $\beta_{\text{len}} \sim \mathcal{N}(1, 0.3)$. The intercept hyperprior $\mu_{\beta_0} \sim \mathcal{N}(-13, 2)$ is a deliberately weak anchor: combined with the exposure terms, a center of -13 places the implied prior crash counts on the order of a few events per segment over the 13-year window, the right order of magnitude for the observed range across functional classes, while the ± 2 prior standard deviation keeps the model from committing to that location and lets the likelihood move it.

Both exposure terms in Eq. (5), length and ADT, carry estimated exponents rather than fixed ones. The natural prior expectation differs between them: segment length is a geometric extent, so doubling a segment’s length might be expected to double the spatial opportunity for a crash ($\beta_{\text{len}} \approx 1$), whereas ADT is a temporal interaction rate for which Hauer (2001) documents a sublinear effect: doubling traffic does not double conflicts because gaps shrink and drivers adjust. We accordingly center both priors at proportionality but estimate both exponents; Section 5.5 shows that the data revise *both* downward, and that the exposure exponent is not even constant across functional classes. This generalization, treating the exposure structure as estimated and class-varying rather than fixed, is the same move the model already makes for the intercept and lane slope, and we arrived at it by model checking rather than by assumption (Section 5.5).

ADT enters the crash likelihood as observed data where measured and as a latent variable where not. For latent ADT, the prior is the ADT submodel posterior predictive given the segment’s covariates; crash counts then feed back into latent ADT through the joint likelihood. A segment with surprisingly many crashes is pulled toward a higher latent ADT (more exposure required to explain the count), which in turn informs the global β_{exp} .

Severing this feedback, as a two-stage approach does, removes the very signal that pins the exposure exponent. The mechanism is identification. On a segment with missing ADT, the only data bearing on its exposure are its covariates and its own crash count. Under joint inference, β_{exp} is identified by the covariation between latent ADT and crash counts across such segments: a high count pulls the latent ADT up, and the magnitude of that pull *is* the exponent. A two-stage pipeline instead imputes each latent ADT from the ADT submodel alone (covariates only) and then freezes it, so the crash likelihood can no longer revise ADT to be consistent with the count it must explain. The frozen imputations are then noisy proxies for the true latent exposure, and a count regression on a noisy regressor attenuates its slope toward zero (classical errors-in-variables), with the intercept rising to keep the mean prediction in place. We confirm this mechanism on simulated data below, where the attenuation is strong enough to bias β_{exp} downward even against a prior centered above the true value.

4.3 Why Joint, Not Two-Stage: A Simulation

Before fitting on real data we ran a generative simulation (Gelman et al., 2020). With $N = 5,000$ segments, 5 functional classes, 10 counties, and parameter values chosen near the posteriors we anticipated, we masked 70% of ADT to mimic the real missingness fraction and fit two competing pipelines on the same simulated data: (i) Bayesian multiple imputation (Rubin, 1987), fitting the ADT submodel separately, drawing $S = 5$ posterior predictive imputations, fitting

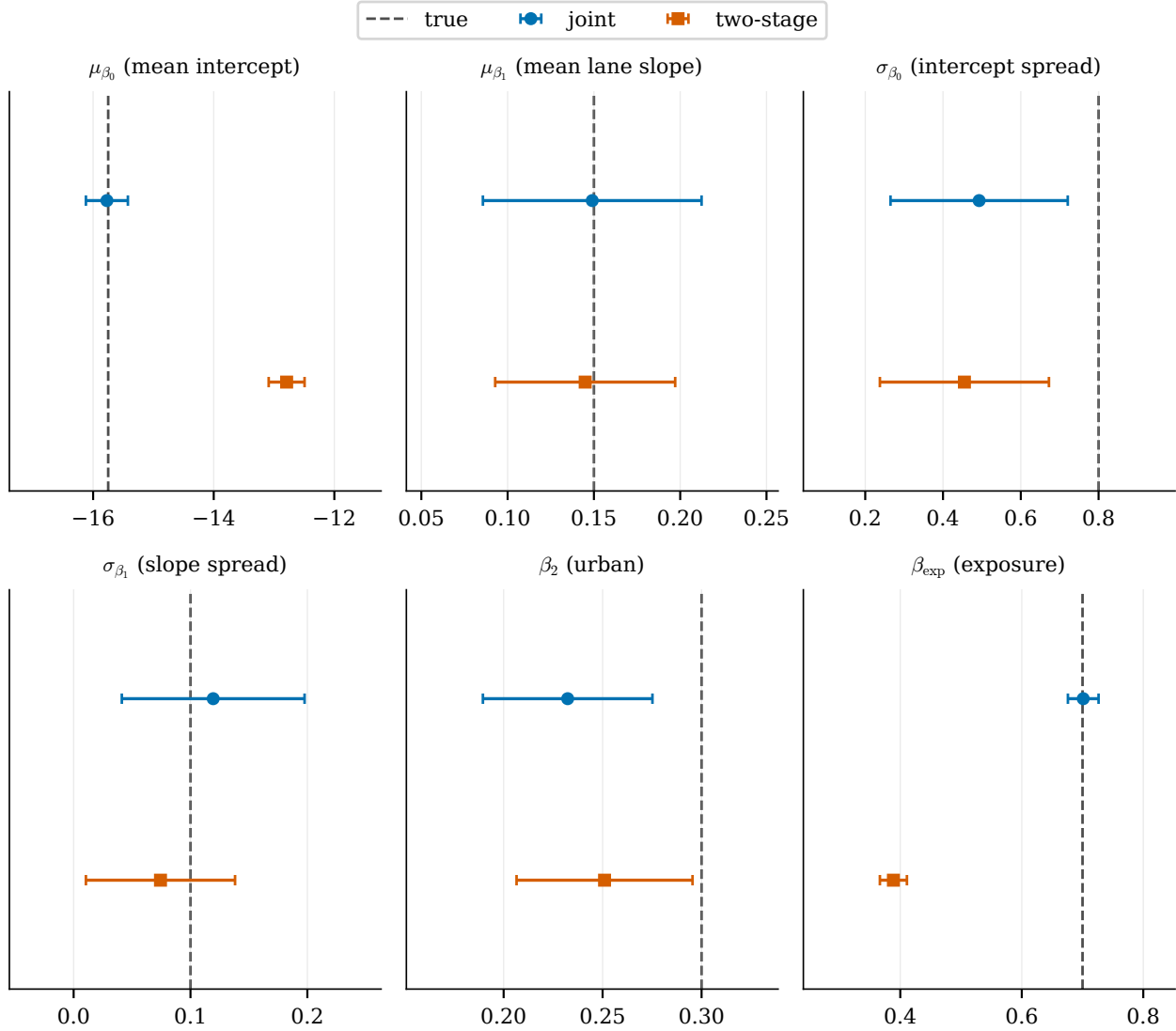


Figure 2: Parameter recovery on simulated data, one self-scaled panel per parameter (the intercept and slopes live on incompatible scales). Dashed line: true value; markers: joint and two-stage posterior means with ± 1 SD. The joint estimates sit on the truth; the two-stage exposure exponent β_{exp} (lower right) is pulled far below it, the attenuation signature of severed crash-to-ADT feedback.

the crash model per imputation, and pooling traces; and (ii) the joint model in which both submodels share inference and the crash likelihood feeds back into the latent ADT.

The joint model recovered the crash-submodel parameters within their posterior credible intervals (Figure 2): the exposure exponent at 0.701 against a true 0.700, with the ADT-noise scale σ_{adt} the lone near-miss (0.829 vs. a true 0.800, a 0.03 overshoot on a parameter estimated to ± 0.015). The two-stage pipeline did not: with a true $\beta_{\text{exp}} = 0.7$, its exposure exponent collapsed to 0.389, a bias of -0.311 , and the intercept μ_{β_0} was biased by $+2.96$, both far outside the joint model’s intervals; worse, the two-stage exponent’s own credible interval is narrow and excludes the truth, so the procedure is not merely biased but confidently wrong. The signs are the ones the attenuation argument predicts: the frozen, covariate-only imputations dilute the exposure signal, pulling β_{exp} below its true value despite a prior centered at 1 that would otherwise pull it up, while the intercept rises to absorb the slack and hold the mean prediction in place.

Joint inference at full scale is computationally infeasible: 408,304 segments include 280,283 latent ADT variables, more than NUTS can sample with practical convergence. We fit on a stratified subsample of 120,468 segments containing 10,000 latent ADT variables. The stratification is by data-availability type, not by a target total. We keep every segment with both measured ADT and crashes (100,468 of them), which carry observed exposure and add no latent parameters,

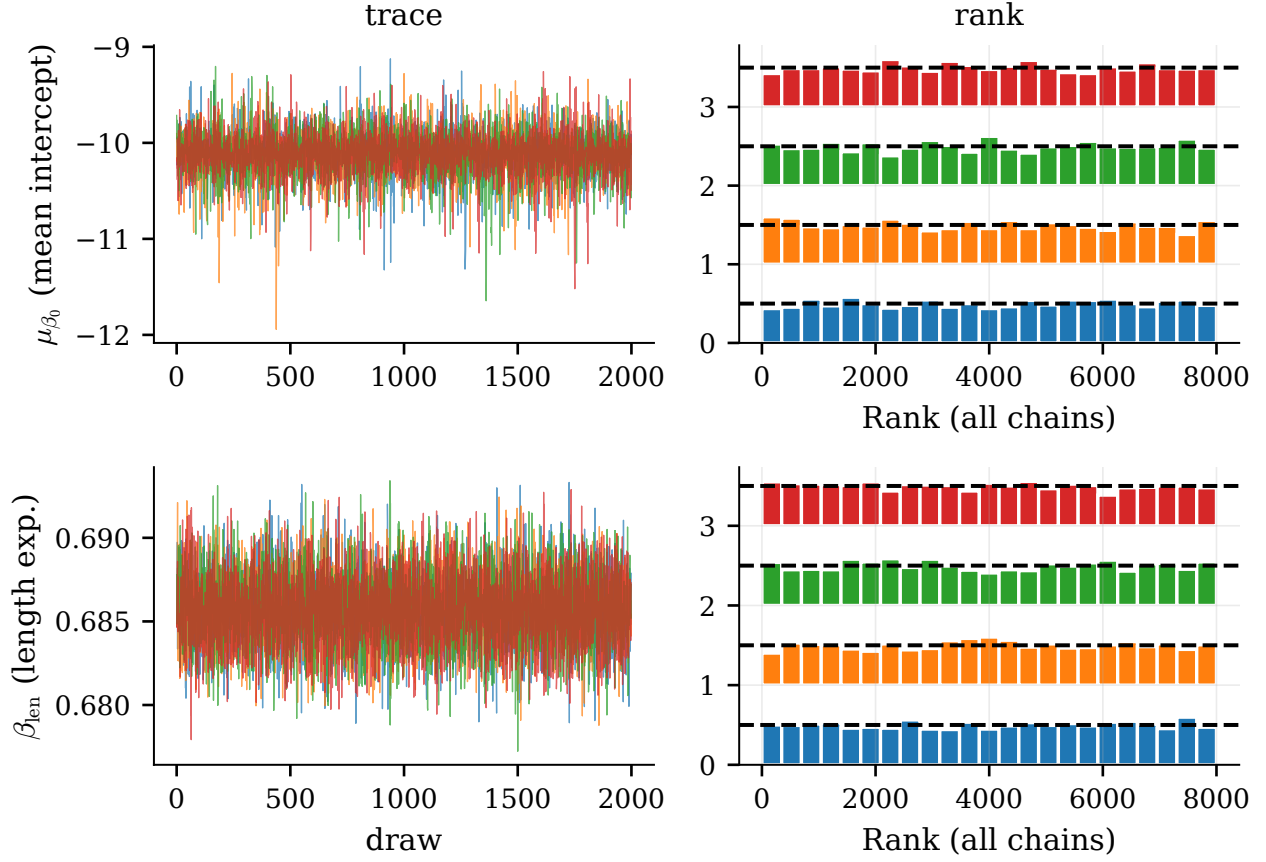


Figure 3: Convergence diagnostics for the two slowest-mixing parameters, β_{exp} and μ_{β_0} . Left: per-chain trace plots; the four chains overlap as a stationary band. Right: rank plots, uniform across chains, confirming good between-chain mixing.

and draw 10,000 each (under a fixed seed) from the missing-ADT-with-crashes and zero-crash strata. The cap binds only on the missing-ADT-with-crashes group: each such segment contributes one sampled latent ADT variable, and that count, not the number of segments, is what governs NUTS cost, with 10,000 the largest we could sample at practical convergence. The zero-crash draw is held to the same size so the informative-zero stratum is represented without overwhelming the likelihood. All three segment types are retained because zeros are informative data, not missing data: a segment with no crashes in 13 years is evidence that it is low-risk. Excluding zeros would condition on crashes > 0 and bias the partial pooling (Hauer et al., 2002). The ADT submodel is also fit on the full 128,021 measured segments separately to provide informed priors for the latent ADT in the joint run.

5 Results

5.1 Convergence and Diagnostics

Both stages converged cleanly (Figure 3): in the joint model the maximum \hat{R} is 1.01 and there were no divergent transitions. The slowest-mixing parameters are the per-FC exposure exponents $\beta_{\text{exp}, \text{fc}}$ and group intercepts $\beta_{0, \text{fc}}$, at bulk ESS ≈ 540 (the expected intercept–slope correlation within a class), while the length exponent β_{len} and the exposure hypermean mix far faster (bulk ESS $> 7,000$) and the latent ADT variables faster still. Pareto- k diagnostics are good for 99.9% of observations; the remaining 124 high-leverage segments are characterized in Section 6.3 rather than removed.

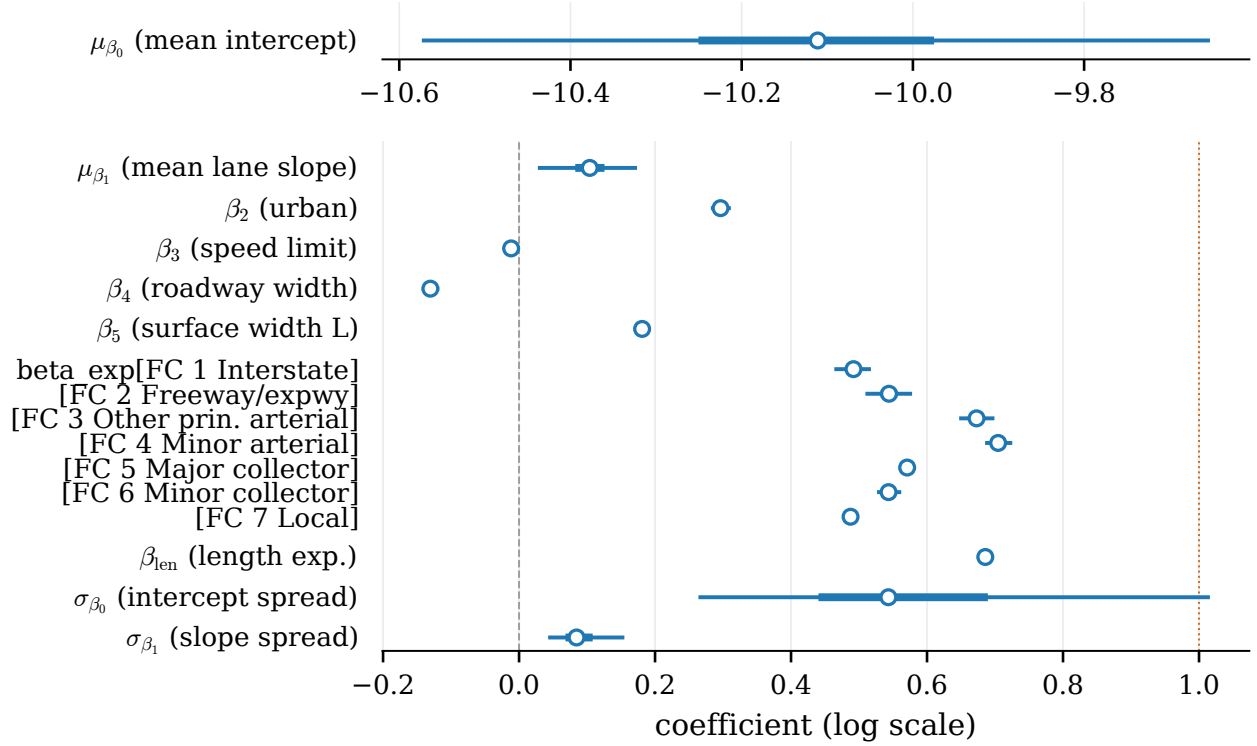


Figure 4: Posterior coefficient estimates with 94% HDIs. The log-rate intercept μ_{β_0} (top panel) is drawn on its own scale; the effect-size coefficients (bottom panel) share a common axis with reference lines at 0 (no effect, dashed) and 1 (proportional exposure, dotted). The seven β_{exp} entries are the per-FC exposure exponents (FC 1–7); they and the length exponent β_{len} all sit well below 1, sublinear in both traffic and length.

5.2 Posterior Estimates and Sublinear Exposure

The headline finding is the exposure structure. Crash count scales *sublinearly* with traffic in every functional class (the safety-in-numbers effect documented by Hauer (2001)), but the strength of the effect varies by class: the per-FC exposure exponent $\beta_{\text{exp}, \text{fc}}$ ranges from 0.49 (interstates and local roads, the flattest) to 0.70 (arterials, the steepest), all well below 1. A single pooled exponent would sit at 0.58 and average this gradient away. Crash count also grows sublinearly with segment *length*: the estimated length exponent is $\beta_{\text{len}} = 0.69$ (94% HDI [0.68, 0.69]), not the proportionality ($\beta_{\text{len}} = 1$) a fixed offset would impose. We arrived at this class-varying, length-estimated exposure structure by model checking (Section 5.5); we do not claim universality, as the exponents are posteriors on Ohio 2013–2025 inventory segments.

The covariate effects sharpen the picture without overturning it (Figure 4). Urban segments carry $\beta_2 = +0.503$ on the log scale (94% HDI [0.488, 0.520]), about 65% higher crash count at fixed exposure, a known but often unquantified urban premium. Higher posted speed limits are associated with *fewer* crashes per segment, $\beta_3 = -0.090$ (HDI [−0.098, −0.083]); this is the access-control signal (high-speed roads are typically grade-separated or have fewer driveways), not a claim about severity, where the sign reverses. Wider total roadways have fewer crashes, $\beta_4 = -0.072$ (HDI [−0.087, −0.059]), consistent with a shoulder and clear-zone effect.

The $\beta_5 = +0.200$ on SURFACE_WIDTH_LEFT (HDI [0.189, 0.212]) is the result that requires explanation rather than defense. The variable measures the paved width on the left of the centerline; in Ohio’s inventory, large values flag divided roads with painted or paved medians. Segments with high left surface width are therefore typically divided arterials with frequent left-turn movements at signalized intersections, high-conflict geometry. The mechanism is not “wider pavement causes crashes” but that the variable acts as a proxy for road type the inventory does not encode directly. We treat the sign as an empirical association, not a design recommendation.

Adding the four fixed-effect covariates to the partial-pooling model narrowed the between-class spread parameters: σ_{β_0} posterior mean fell from 0.65 (3-covariate model) to 0.60 (6-covariate), and σ_{β_1} from 0.14 to 0.12. Variance previously attributed to between-FC differences is now explained by within-FC covariates.

Table 1: PSIS-LOO comparison of model variants on the joint-model subsample. Lower elpd_{100} indicates a worse model; p_{100} is the effective parameter count. Pareto- k counts segments with $k > 0.7$. The two complete-pooling rows use the scalar-exposure, fixed-offset crash structure, so the partial-vs-complete contrast is made on a common structure; the exposure generalization is assessed separately in the top two rows.

Model	elpd_{100}	SE	p_{100}	Pareto- $k > 0.7$
6-cov, partial pooling	-391,783	704	1,427	151
3-cov, partial pooling	-392,768	701	1,466	177
6-cov, complete pooling	-396,563	728	41	1
3-cov, complete pooling	-399,600	709	12	0

Table 2: Posterior mean crash rate per million VMT by functional class, on measured-ADT segments, with within-class standard deviation, minimum, and maximum across segments. The rate is predicted crashes divided by actual vehicle-miles travelled, exposure-normalized and invariant to the exposure parameterization. Rates are point posterior means of segment-level distributions; per-segment uncertainty is omitted for compactness.

FC	Class	Mean	SD	Min	Max
1	Interstate	1.63	1.43	0.13	27.3
2	Freeway / expressway	1.67	1.30	0.19	21.5
3	Other principal arterial	5.10	3.29	0.54	66.6
4	Minor arterial	4.95	3.19	0.50	43.8
5	Major collector	4.77	3.69	0.42	151.0
6	Minor collector	5.74	4.97	0.85	92.5
7	Local	5.94	6.22	0.36	233.5

5.3 Model Comparison

We compare model variants by PSIS-LOO (Vehtari et al., 2017) (Table 1): the headline model with a per-FC exposure exponent and an estimated length exponent (Section 5.5); its scalar-exponent, fixed-offset predecessor; the 3-covariate partial-pooling model; and complete-pooling counterparts at both covariate counts. Each comparison below isolates one modeling axis.

Pooling. On a common crash structure, partial pooling beats complete pooling by $\Delta\text{elpd} = 4,780$ (SE 225), a margin much larger than its uncertainty. *Covariates.* The 6-covariate model beats the 3-covariate version by 985 elpd with a lower effective parameter count (1,427 vs. 1,466): the added covariates carry independent signal, not just complexity. *Exposure structure.* Generalizing the fixed exposure assumptions, replacing one scalar and a fixed offset with a per-FC exponent and an estimated length exponent, improves elpd by a further 9,394 (SE 238), the largest single gain in the table, while *reducing* both the effective parameter count (1,154 vs. 1,427) and the high- k count (124 vs. 151). It is a strictly better fit, not a more flexible one; Section 5.5 shows the posterior predictive checks that motivated it.

We do not include a no-pooling baseline. With 7 well-populated functional class groups, independent per-FC fits would be a strawman; the substantive question is whether the data support sharing strength across classes (partial vs. complete pooling), and the answer is unambiguous.

5.4 Posterior Crash Rates

Posterior mean crash rates per million vehicle miles travelled (VMT), defined as predicted crashes divided by actual VMT and averaged within each functional class, are shown in Table 2, with Fig. 5 showing the segment-level shrinkage behind them. The rates order as exposure intuition predicts: limited-access facilities are safest per mile travelled (interstates at 1.6 and freeways/expressways comparable), while collectors and local roads run highest (local at 5.9, other principal arterials at 5.1). The within-class spread is wide (a handful of segments per class run several times the class mean), which is exactly the segment-level heterogeneity the partial-pooling crash submodel and the per-FC exposure exponent estimate rather than assume away.

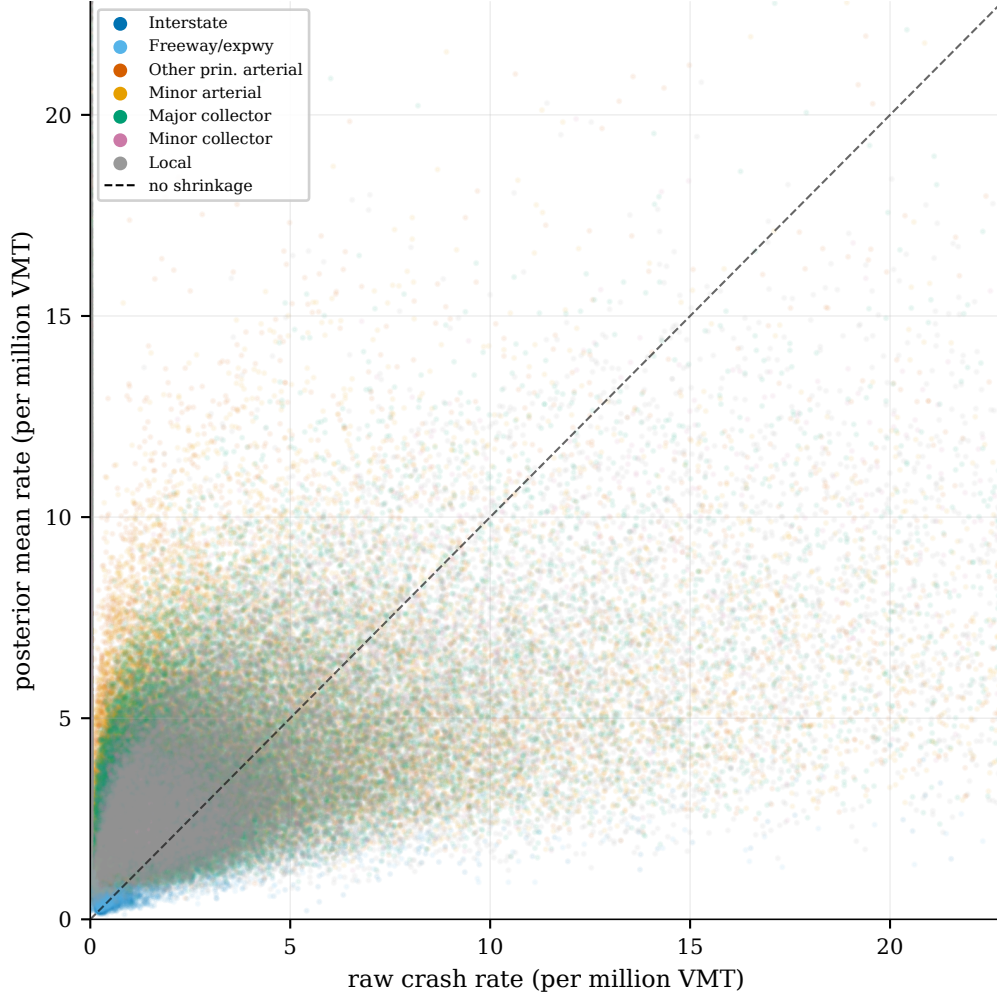


Figure 5: EB-style shrinkage on measured segments: raw crash rate (crashes per million VMT) versus the model’s posterior mean rate, by functional class. Sparse-data segments are pulled off the no-shrinkage diagonal toward their class mean; data-rich segments stay near it. This is the Bayesian analogue of Hauer’s EB weighting, Eq. (1), with the weight learned rather than fixed.

5.5 Posterior Predictive Checks and Model Expansion

The class-varying, length-estimated exposure structure of Eq. (5) was not assumed; it was arrived at by checking a simpler model and expanding where the checks failed, in the manner of Gelman et al. (2020). We describe that path here, because it both motivates the structure and demonstrates the paper’s thesis in miniature.

The standard model and its misfit. We began with the field-standard specification: a single exposure exponent β_{exp} and segment length as a fixed offset (exponent 1), exactly the form an HSM-style safety performance function takes. Posterior predictive checks compare simulated crash counts to observed counts along four marginal views: the overall count distribution (log scale, for the heavy zero mass and long tail), and means by functional class, by ADT decile, and by segment-length quintile. The overall distribution and the per-class means track the data, but the two exposure-facing panels reveal a systematic over-prediction that grows at the tails: predicted means run about $1.4\text{--}1.6\times$ observed in the upper ADT deciles and the longest-segment quintile (Figure 6).

Diagnosis. The two tail misfits are not redundant. Length and ADT are negatively correlated across segments (long segments are disproportionately rural and low-traffic), so a single confounded effect would bias the two panels in opposite directions, not the same one. Instead each panel implicates a distinct fixed assumption: the ADT-decile bias

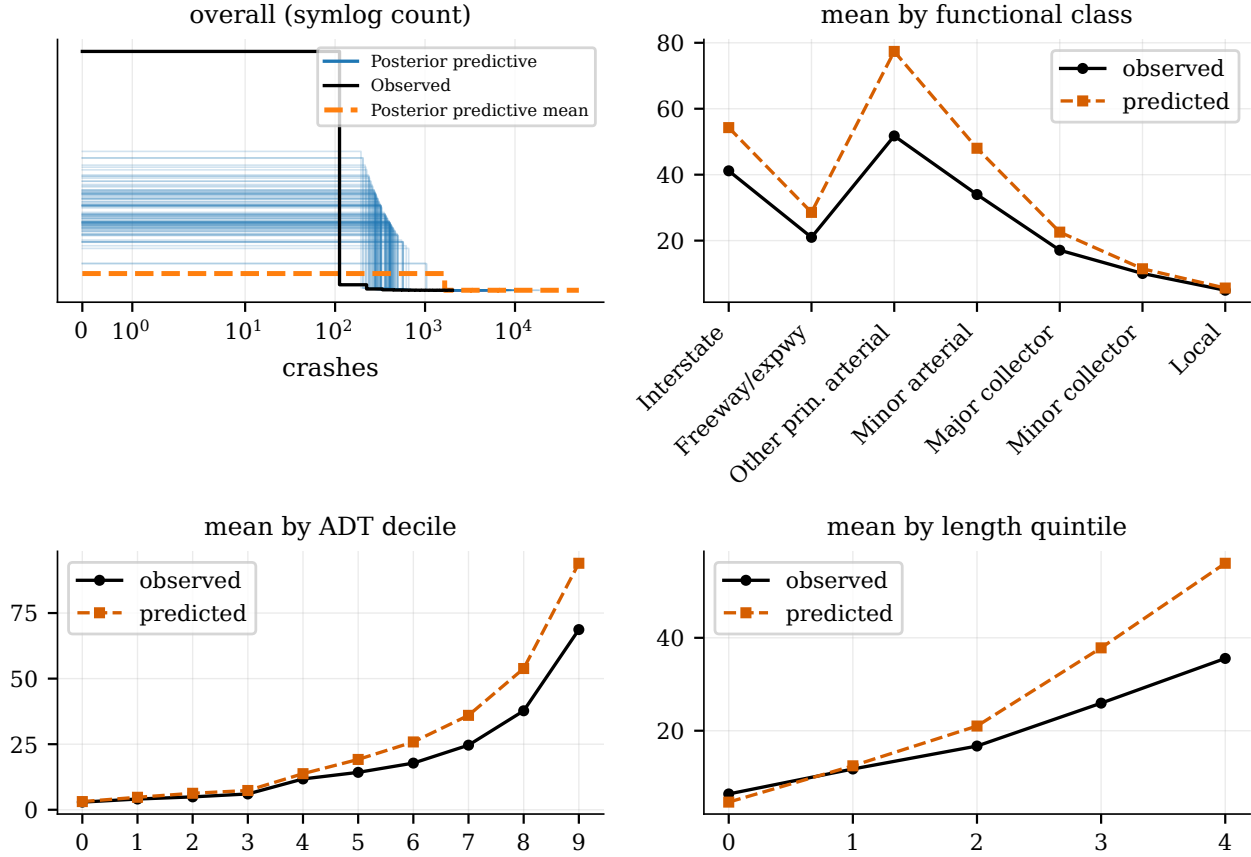


Figure 6: Standard-model posterior predictive checks (single exposure exponent, fixed length offset). (i) Overall count distribution on a symmetric-log scale; (ii)–(iv) observed versus posterior-predictive mean counts by functional class, ADT decile, and segment-length quintile. The per-class means track, but predicted means over-predict by 1.4–1.6 \times in the upper ADT deciles and the longest-segment quintile, the misfit that motivates the exposure expansion.

points at the single scalar exponent, which cannot bend across the traffic range, and the length-quintile bias points at the exponent-one offset, which over-credits exposure on long, homogeneous, low-conflict rural mainline.

Expansion and re-check. We relaxed exactly those two assumptions, letting β_{exp} vary by functional class under a shared hyperprior and estimating the length exponent β_{len} (Eq. (5)), the same partial-pooling move the model already applies to the intercept and lane slope. The expansion is decisively supported: $\Delta\text{elpd} = 9,394$ (SE 238) over the standard model (Table 1), with a *lower* effective parameter count and fewer high-leverage segments: a better fit, not merely a more flexible one. The data revise both exponents below proportionality ($\beta_{\text{len}} = 0.69$; per-FC β_{exp} from 0.49 to 0.70, Fig. 4), and the two are cleanly identified: their posterior correlation is below 0.1 despite the length–ADT collinearity, so this is a genuine decomposition rather than a trade-off. Re-running the checks on the expanded model closes the gap: predicted and observed means coincide across all three groupings, and within-class calibration tightens to within a few percent of parity (Figure 7).

5.6 Held-Out Year Validation

The 13-year crash window assumes road characteristics and crash-reporting practice are approximately stationary. A natural check, which we leave to future work, refits the joint model on 2013–2022 and evaluates predictive performance on 2023–2025, asking whether β_{exp} and the FC-level mean rates are stable when held-out years are dropped from fitting. Stability would not prove stationarity but would weaken the argument against it; we expect it to be a more substantive robustness check than a no-pooling baseline.

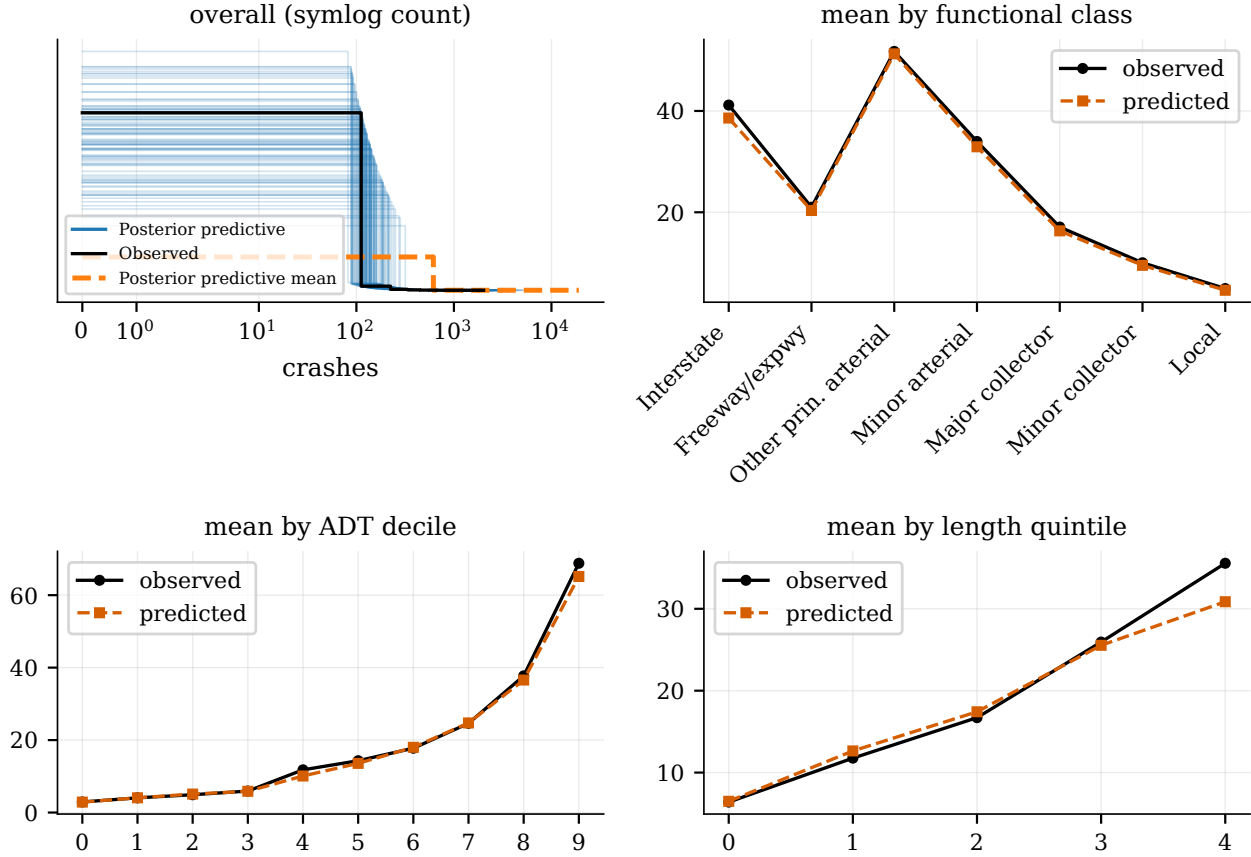


Figure 7: Expanded-model posterior predictive checks (per-FC exposure exponent, estimated length exponent), same four views as Fig. 6. Predicted and observed means now coincide across functional class, ADT decile, and segment-length quintile; the tail over-prediction is resolved.

Table 3: Correspondence between Empirical Bayes fixed-parameter assumptions and the present model’s relaxations.

EB assumption	Bayesian generalization
SPF coefficients (α, β) are MLE point estimates fit at calibration	Joint posterior over all coefficients, propagated end-to-end into segment rates
Overdispersion ϕ is one number per road type	Per-FC overdispersion α_{fc} estimated jointly with the SPF coefficients
ADT is observed	Latent variable where missing, joint with the crash likelihood so counts inform exposure
Exposure exponent fixed at SPF calibration	Estimated and partially pooled across functional class ($\beta_{exp, fc}$ from 0.49 to 0.70); segment length likewise carries an estimated exponent $\beta_{len} = 0.69$
Output is the point estimate $\hat{\lambda}^{EB}$	Full posterior $p(\lambda_i \text{data})$ per segment

6 Discussion

6.1 What the Model Generalizes

Table 3 maps each fixed-parameter assumption from the EB recipe to its generalization in the present model. Read down the left column for the EB-fluent description and across to the right for the change.

6.2 When Empirical Bayes Remains Appropriate

EB remains the right tool when its assumptions hold. Where ADT is broadly observed, where road types within a class are homogeneous, where point estimates suffice for the application, and where practitioner accessibility outweighs uncertainty quantification, EB delivers most of the same shrinkage at a fraction of the computational and methodological cost. The present model adds value where these conditions strain, in particular when ADT is missing on a majority of segments and the downstream application consumes a distribution rather than a number. We mean this seriously: the spreadsheet workflow EB enables is a feature of the method that no MCMC sampler will replace for many of the audiences EB serves.

6.3 Limitations

Several limitations bear stating prominently rather than burying.

The ADT submodel shows regression-to-the-mean bias at the tails of the ADT distribution: low-ADT segments are over-predicted and high-ADT segments under-predicted, as expected at $R_{\log}^2 = 0.76$. The bias is smaller than LightGBM’s on equal features (residual range $[-1.14, +0.37]$ vs. $[-1.31, +0.71]$ on the log scale) but real. Wider posteriors on extreme segments propagate the uncertainty honestly; they do not eliminate the bias. Closing it would require features not available in the inventory, in particular access control and intersection density.

The exposure expansion of Section 5.5 resolves the tail over-prediction in aggregate, but a second-order residual remains: split by urban/rural, the expanded model still over-predicts mean crashes by roughly 20–30% on rural *mid*-length segments, even as it calibrates well on urban segments and at both length extremes. The likely cause is the same missing covariates noted above (access control and intersection density), which are concentrated on exactly those roads. A length exponent that varied by class, or an explicit length-by-class interaction, could absorb it; we leave that to future work rather than add structure the diagnostics only weakly demand.

A small set of segments, 124 of $\sim 120,000$ (0.10%), have Pareto- $k > 0.7$, indicating the LOO importance weights are heavy-tailed and the elpd contribution is unreliable for those points. We do not remove them; they are the cases where the model is least sure, and the correct response is to characterize them rather than paper over them (Figure 8).

The covariate set excludes three variables that the Highway Safety Manual emphasizes (access control, median type, and intersection density) because they are not in the inventory extract. The model estimates predictive associations within functional class and the available covariates; it should not be read as an estimate of pure causal effects. The new covariates ($\beta_3, \beta_4, \beta_5$) partially substitute for these missing differentiators but do not replace them.

ADT is assumed missing at random conditional on the road attributes in the ADT submodel. This is plausible (DOT counting programs prioritize higher-class roads, and functional class is in the model) but unverifiable. Residual selection within functional class would bias the latent ADT estimates, and consequently β_{exp} , in the direction of the selection.

The sign on β_5 (left surface width) requires domain validation. We have offered a mechanism (proxy for divided-road geometry); a Highway Safety Manual specialist may have a cleaner interpretation. We do not adjust the model on the strength of an interpretation alone.

The data come from a single state and a 13-year window. Replication on another DOT’s inventory is the cleanest test of generalizability and is left as future work.

6.4 Integration with Risk-Aware Routing

The output of this model is a posterior crash rate distribution per inventory segment. In the routing framework of Skaug and Nojournian (2026), percentile-based risk scores are replaced by posterior means and route-level aggregation can report credible intervals rather than point estimates, the first time, to our knowledge, that route-level risk in this pipeline can carry honest uncertainty bands. The integration with the GraphHopper-based routing pipeline is in progress; we defer the corridor demonstration to a routing-focused follow-up to keep the present paper’s scope on the Bayesian generalization itself. Related in-vehicle safety systems developed alongside this routing work, covering road-risk awareness and sun-glare avoidance for semi- and fully autonomous driving, are described in pending patents (Nojournian and Skaug, 2025a,b).

7 Conclusion

We presented a Bayesian hierarchical model that generalizes Hauer’s Empirical Bayes procedure by relaxing each of its fixed-parameter assumptions in a single joint inference. Model checking drove the central refinement: posterior

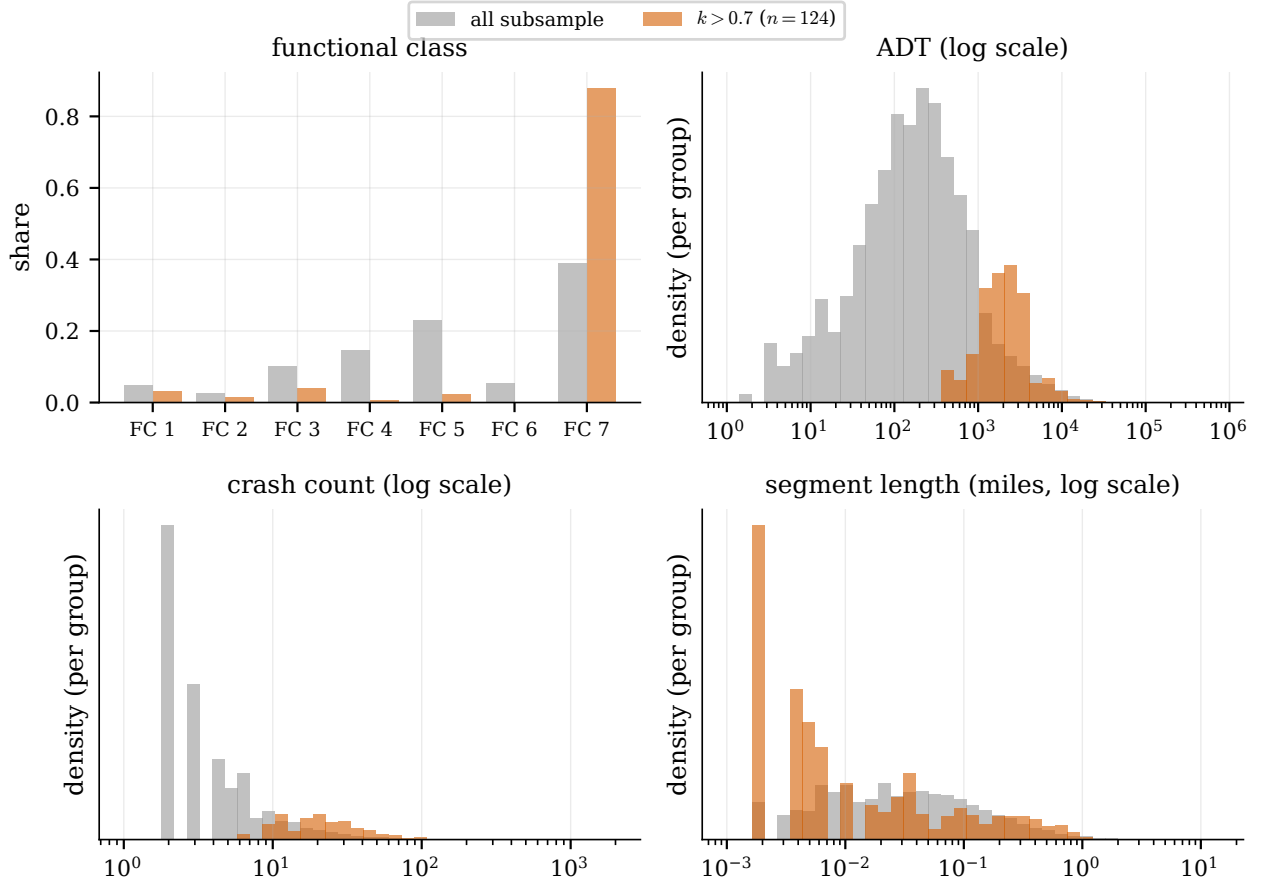


Figure 8: Characterization of the high-Pareto- k segments (the 124 with $k > 0.7$ in the expanded model), overlaid on the full joint subsample across functional class, ADT, crash count, and segment length (the latter three on log scales). Each group is normalized to unit area, so the panels compare distribution shape rather than counts, the high- k group being far smaller. These are the segments where the model is least sure; rather than remove them we show what distinguishes them: they are overwhelmingly local roads (FC 7) at higher ADT and crash counts than the subsample, concentrated at short-to-mid lengths and lacking the longest segments.

predictive checks of a fixed-exposure model exposed a tail misfit, and relaxing the exposure structure to a per-functional-class exposure exponent and an estimated length exponent resolved it. Crash count is sublinear in both traffic and length, the safety-in-numbers regime, but now as class-varying posterior intervals rather than chosen values. Each segment receives a posterior crash rate distribution that propagates ADT uncertainty end-to-end, suitable for downstream consumers, including routing applications, that benefit from intervals over points. EB remains appropriate where its assumptions hold; the contribution here is computational evolution, not correction.

Data Availability

The road inventory, traffic count segments, and crash records used in this study are public datasets from the Ohio Department of Transportation. The model is specified in full in Section 4.

Acknowledgments

The author thanks Mehrdad Nojournian, who advised the prior work (Skaug and Nojournian, 2026) on which this paper builds.

References

- Hauer, E., Harwood, D.W., Council, F.M., and Griffith, M.S. (2002). Estimating Safety by the Empirical Bayes Method: A Tutorial. *Transportation Research Record* 1784, 126–131.
- Hauer, E. (2001). Overdispersion in Modelling Accidents on Road Sections and in Empirical Bayes Estimation. *Accident Analysis & Prevention* 33, 799–808.
- Skaug, L. and Nojournian, M. (2026). Risk-Aware Navigation Framework for Autonomous and Human-Driven Vehicles: Integrating Crash Probability Data for Safer Mobility. *SAE International Journal of Connected and Automated Vehicles* 9(3), Article 12-09-03-0019. doi:10.4271/12-09-03-0019.
- Skaug, L., Nojournian, M., Dang, N., and Yap, A. (2025). Road Crash Analysis and Modeling: A Systematic Review of Methods, Data, and Emerging Technologies. *Applied Sciences* 15(13), 7115. doi:10.3390/app15137115.
- Skaug, L. and Nojournian, M. (2025). A Multimodal Artificial Intelligence Framework for Intelligent Geospatial Data Validation and Correction. *Inventions* 10(4), 59. doi:10.3390/inventions10040059.
- Nojournian, M. and Skaug, L. (2025). Road-Risk Awareness System (RAS) in Semi or Fully Autonomous Vehicles. U.S. Patent Application 19/016,485 (pending).
- Nojournian, M. and Skaug, L. (2025). Sun Glare Avoidance System (SAS) in Semi or Fully Autonomous Vehicles. U.S. Patent Application 19/016,240 (pending).
- Gelman, A. and Hill, J. (2007). *Data Analysis Using Regression and Multilevel/Hierarchical Models*. Cambridge University Press.
- Vehtari, A., Gelman, A., and Gabry, J. (2017). Practical Bayesian Model Evaluation Using Leave-One-Out Cross-Validation and WAIC. *Statistics and Computing* 27, 1413–1432.
- Gelman, A., Vehtari, A., Simpson, D., et al. (2020). Bayesian Workflow. *arXiv:2011.01808*.
- Rubin, D.B. (1987). *Multiple Imputation for Nonresponse in Surveys*. Wiley.